Journal of Hazardous Materials 381 (2020) 120917

Contents lists available at ScienceDirect

Journal of Hazardous Materials

journal homepage: www.elsevier.com/locate/jhazmat

Facile method to synthesize efficient adsorbent from alumina by nitric acid activation: Batch scale defluoridation, kinetics, isotherm studies and implementation on industrial wastewater treatment

Usha Kumari[a,*], Sushanta K. Behera[a], Hammad Siddiqi[a], B.C. Meikap[a,b]

[a] Department of Chemical Engineering, Indian Institute of Technology (IIT) Kharagpur, West Bengal 721302, India
[b] Department of Chemical Engineering, School of Chemical Engineering, Howard College Campus, University of Kwazulu-Natal (UKZN), Durban 4041, South Africa

GRAPHICAL ABSTRACT

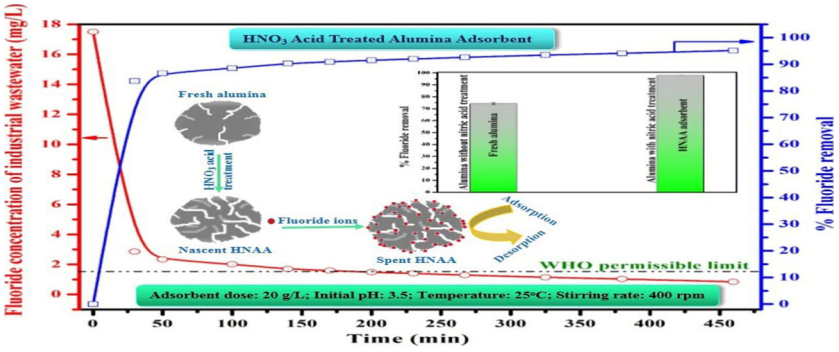

ARTICLE INFO

Editor: Deyi Hou

Keywords:
Fluoride adsorption
Acid activated alumina
Industrial wastewater treatment
Nitric acid

ABSTRACT

The excess amount of fluoride contamination in the groundwater or industrial effluents fosters various health problems. Considering the advantages of adsorption, the current research reports the synthesis of a novel adsorbent (HNAA) by simple and convenient process of nitric acid activation of alumina. The physiochemical characterization (SEM, EDX, XRF, FTIR, BET, and pH_{ZPC}) results exhibited successful activation of alumina and adsorption of fluoride ions. The effect of process parameters (contact time, initial pH, adsorbent dose, initial fluoride concentration and presence of coexisting ions) on adsorption of fluoride ions on HNAA were investigated in batch scale. The adsorption of fluoride ion on HNAA followed the Freundlich isotherm and pseudo second order kinetic model. The Q_{max} of HNAA adsorbent was 45.75 mg/g at 45 °C. The fluoride ion adsorption was revealed to be endothermic and spontaneous. The experimentation of the HNAA adsorbent on industrial wastewater, with fluoride concentration of 17.5 mg/L, inferred the significant defluoridation potential at the optimized adsorbent dose and pH. The nitric acid activation of alumina resulted in improvement of defluoridation efficiency from 74.18% to 97.43%. The HNAA also exhibited the better regeneration and reusability features which distinguish it as a promising adsorbent to be applied for real field wastewater.

* Corresponding author at: Indian Institute of Technology (IIT) Kharagpur, West Bengal, 721302, India.
E-mail address: usha.kumari@iitkgp.ac.in (U. Kumari).

https://doi.org/10.1016/j.jhazmat.2019.120917
Received 9 April 2019; Received in revised form 19 July 2019; Accepted 22 July 2019
Available online 25 July 2019

1. Introduction

Drinking water with minute amount of fluoride is requisite for the healthy growth of humans and animals. The low concentration of fluoride plays a crucial role in the normal mineralization of bone and development of dental enamels (Fan et al., 2003). But, the unlimited consumption of fluoride ions through drinking water has the adverse effect like cancer, fluorosis (skeletal, crippling and dental), Alzheimer syndrome, infertility, arthritis, brain damage, and thyroid (Naim et al., 2012). The high concentration of fluoride ions in drinking water is a serious concern in the countries of Asia and South Africa (e.g. China, India, Sri Lanka, Ghana, etc.). India is reported to be 23rd nation in the world where the problem of fluorosis has engraved a large population of the country (Biswas et al., 2009; Guler and Thyne, 2004). The contamination level of fluoride ions in drinking water, in India, has reached up to the range of 1.58–37 mg/L (Meenakshi and Maheshwari, 2006). The persistent cause of fluoride ions contamination in drinking water is both the natural (e.g., rock weathering and volcanic eruption) and anthropogenic actions (e.g., industrialization, urbanization, coal combustion, fertilizer application in agriculture, fly ash disposal, etc.). The wastewater effluent from industries like aluminum, semiconductor, and pesticide contains high concentration of fluoride which is hazardous to discard in the open environment. Such type of industries affect the fluoride level in the groundwater which is a major source of drinking water. To raise awareness about fluoride contamination in drinking water, the WHO (World Health Organization) has recommended the maximum allowable limit of 1.5 mg/L of fluoride concentration in drinkable water (WHO, 2006; Dong and Wang, 2016). Therefore, it is essential to develop efficient, convenient and economically viable technology to reduce high fluoride concentration level in wastewater effluent from industrial sources or groundwater.

Various technologies have been attempted by researchers for the defluoridation from wastewater such as ion-exchange, electrocoagulation, electrochemical technique, adsorption, Donnan dialysis, and membrane separation (Bhatnagar et al., 2011; Nie et al., 2012a; Asgari et al., 2012). The adsorption method of fluoride removal is considered to be better than the other reported technologies. It is because of its simple operation, low cost, easy availability and ecofriendly nature. Considering these advantages of adsorption, a large number of adsorbents had been tested like bio-adsorbent, chitosan, bone char, calcite, layered double hydroxide, Plaster of paris, zeolites, and polymeric materials (Bhatnagar et al., 2011). Although they are capable of removing fluoride from aqueous solution, the shortcomings of such adsorbents are low adsorption capacity to fluoride ions, cumbersome/time-consuming synthesis process, and expensive to implement. All these limitations make such adsorbents impractical for actual application in the fluoride affected rural areas and industrial effluents.

The electropositive nature of metal oxides is known for better adsorption of fluoride ions. One such example of metal oxide is alumina (Bhatnagar et al., 2011). The application of alumina is also recommended by the USEPA (United State Environmental Protection Agency) for defluoridation in the fluoride affected regions (USEPA, 2003). Additionally, the defluoridation researches have gained more attention toward the selection of alumina adsorbent because of its high selectivity and affinity to fluoride ions (Bhatnagar et al., 2011; Kumar et al., 2011).

Various researches have been attempted for the removal of fluoride ions by using alumina and commercial activated alumina adsorbents (Ghorayi and Pant, 2004; Ku and Chiou, 2002). But, these adsorbents have low adsorption capacity to fluoride ions. Therefore, the modifications in the adsorptive property of alumina have been attempted. Researches were reported for the application of oxidizing acids for acidic activation of adsorptive materials to increase their adsorption capacity (Wang and Zhu, 2007; El-Hendawy, 2003; Gokce and Aktas, 2014; Dutta et al., 2011). However, very limited attempt was given for acid activation of alumina as adsorptive material for fluoride removal. Literature survey also evidenced that acid treatment of alumina alters its adsorptive and catalytic properties (Gong et al., 2012). Considering these facts, Wu et al. (2010) have applied the HCl acid for acid activation of alumina and utilized it for removal of fluoride ions from wastewater (Chen et al., 2010a). But, it also has the limitation of low adsorption capacity of fluoride (0.89 mg/g) and very long treatment time (50 h). No research was attempted for the acid activation of alumina by using HNO_3 acid which is known for its strong oxidizing nature. Hence, the application of nitric acid activated alumina adsorbent for defluoridation is still the unexplored area of research. Besides, the utilization of nitric acid treated alumina has not been reported for treatment of fluoride contaminated industrial wastewater. Therefore, the present research is focused on the modification of adsorptive property of alumina by nitric acid treatment and examination of its fluoride removal potential.

In this study, an adsorbent for fluoride removal was synthesized by acid activation of alumina by using nitric acid. The experiments were carried out on the batch scale to know the defluoridation properties of the adsorbent. The attempt was made to explore the factors affecting the adsorption of fluoride ions on the adsorbent like initial pH, adsorbent dose, contact time, initial fluoride concentration and presence of coexisting ions. Besides, the isotherm, kinetics, thermodynamic studies were conducted. Various characterizations of the prepared adsorbent were carried out to analyze the physiochemical properties. The defluoridation performance of the adsorbent was investigated for industrial wastewater treatment. For the reuse of adsorbent the regeneration study was also conducted.

2. Materials and methods

2.1. Materials

Alumina was brought, for experimental investigation, from the aluminum industry of Odisha, India. The chemicals (i.e., NaF, HCl, HNO_3, NaOH, Na_2SO_4, $NaHCO_3$, $NaNO_3$, NaCl and Na_2CO_3) applied in the experiments were of AR grade. All chemicals were purchased from Merck Ltd., Mumbai, India. The supplier of the chemicals was M/s, Anupam Enterprise, Kharagpur, India. The double distilled water utilized in the experimentation was facilitated by the departmental research facility of IIT Kharagpur, India.

2.2. Adsorbent preparation

The nitric acid was added to alumina in the volume (HNO_3; mL) to weight (alumina; g) ratio of 1:1 (v/w). The acid was thoroughly blended with alumina by manual stirring to make a thick slurry. Precaution was taken to avoid fume exposure during mixing. The acidification period of alumina was continued for 30 min (Kumari et al., 2019). After 30 min, the sample was washed thoroughly with water to remove excess nitric acid. The sample was placed in the hot air oven (105 °C) for elimination the moisture content (Fig. 1). The dried sample, dubbed as HNAA, was stored in airtight container for restriction of environmental contamination.

2.3. Synthetic wastewater preparation and analysis

The synthetic wastewater was utilized to explore the adsorptive nature of HNAA. Therefore, synthetic wastewater (1000 mg/L) of fluoride was prepared in stock by adding 2.21 g of NaF in 1 L of double distilled water. The successive dilution method was applied to prepare the desired concentration of fluoride from the stock solution. The instrument applied to measure the concentration of fluoride ions was ion selective electrode (Orion 720A+, Thermo electron corporation, Beverly, USA). The TISAB III was added to the analyzing sample in the volume ratio ($V_{TISAB\ III}/V_{aq.\ sample}$) of 1:10.

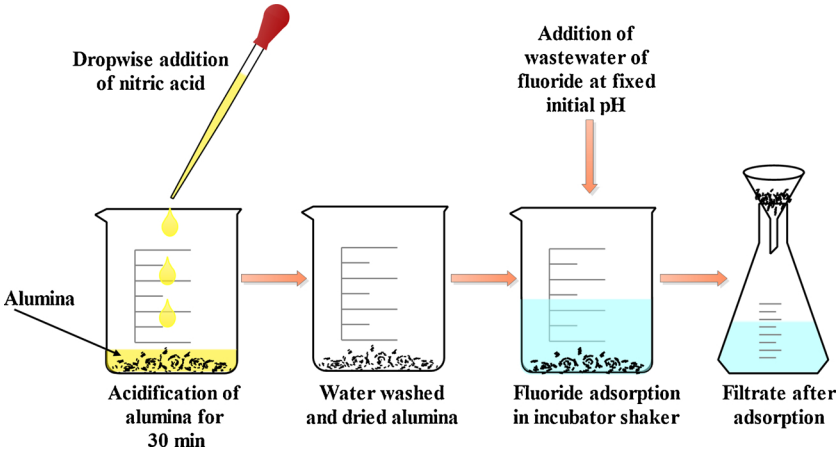

Fig. 1. Description of experimental procedure.

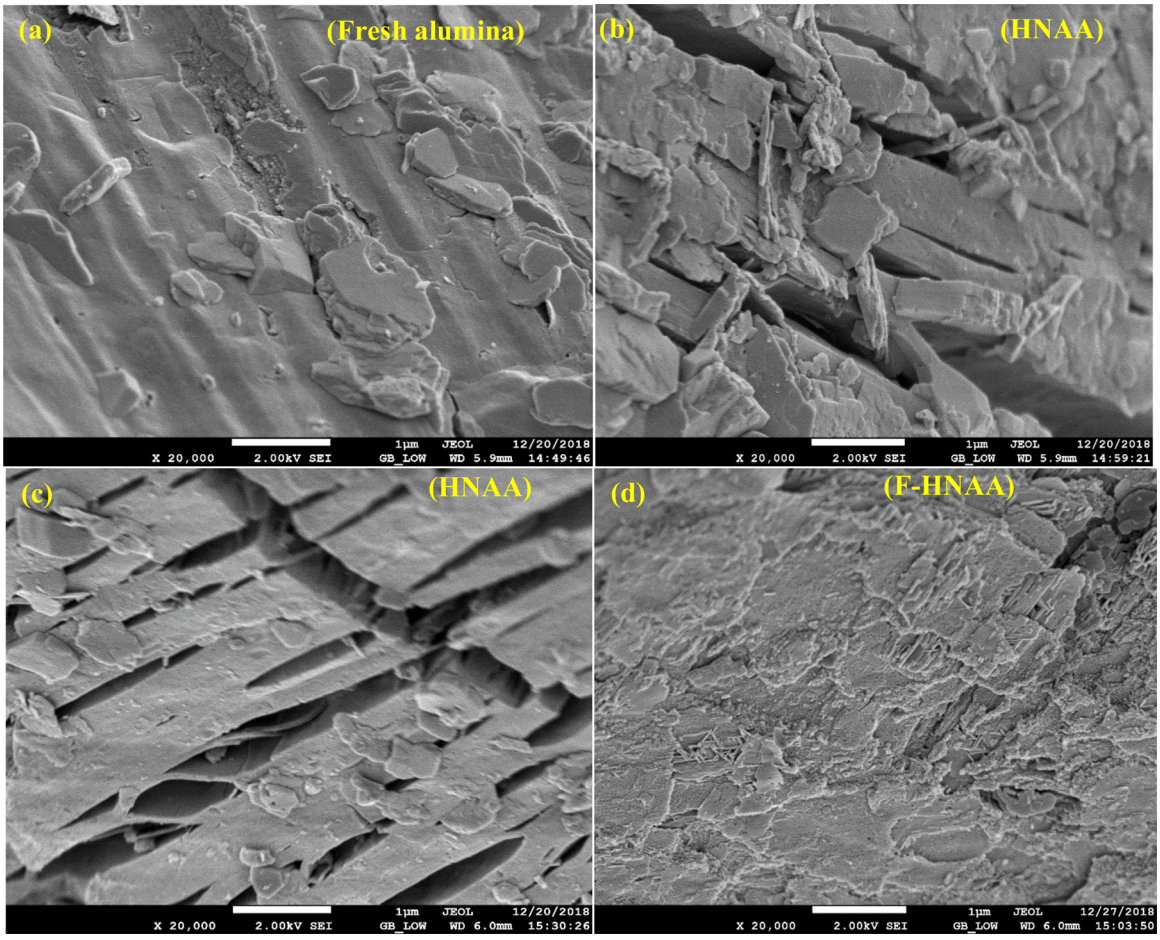

Fig. 2. SEM analysis (20,000 × magnification) of (a) fresh alumina, (b) and (c) nascent nitric acid treated alumina adsorbent (HNAA) (d) spent HNAA adsorbent (F-HNAA).

2.4. Adsorption experiments

Each adsorption experiment was conducted in the 250 mL glass beaker containing 100 mL of fluoride solution (Fig. 1). The incubator shaker fitted with temperature controller was used to conduct the experiments. The dilute solution of HCl and NaOH were applied for the pH adjustment of the adsorbate solution. The estimation of Q_e (equilibrium adsorption capacity) and percent fluoride removal was achieved by Eq. (S1) and (S2), respectively (Supplementary Material).

2.5. Characterizations of HNAA adsorbent

The Scanning electron microscope (SEM) and energy dispersive X-ray (EDX) analysis of the samples were conducted to achieve the surface morphology and elemental chemical composition, respectively. The N_2 adsorption-desorption isotherm and specific surface area of the samples were obtained by Bruanauer-Emmette-Teller (BET) analysis. The functional groups present on the surface of adsorbent samples were analyzed by the application Fourier transform infrared spectroscopy (FTIR). The Thermogravimetric (TGA) analysis of the alumina samples

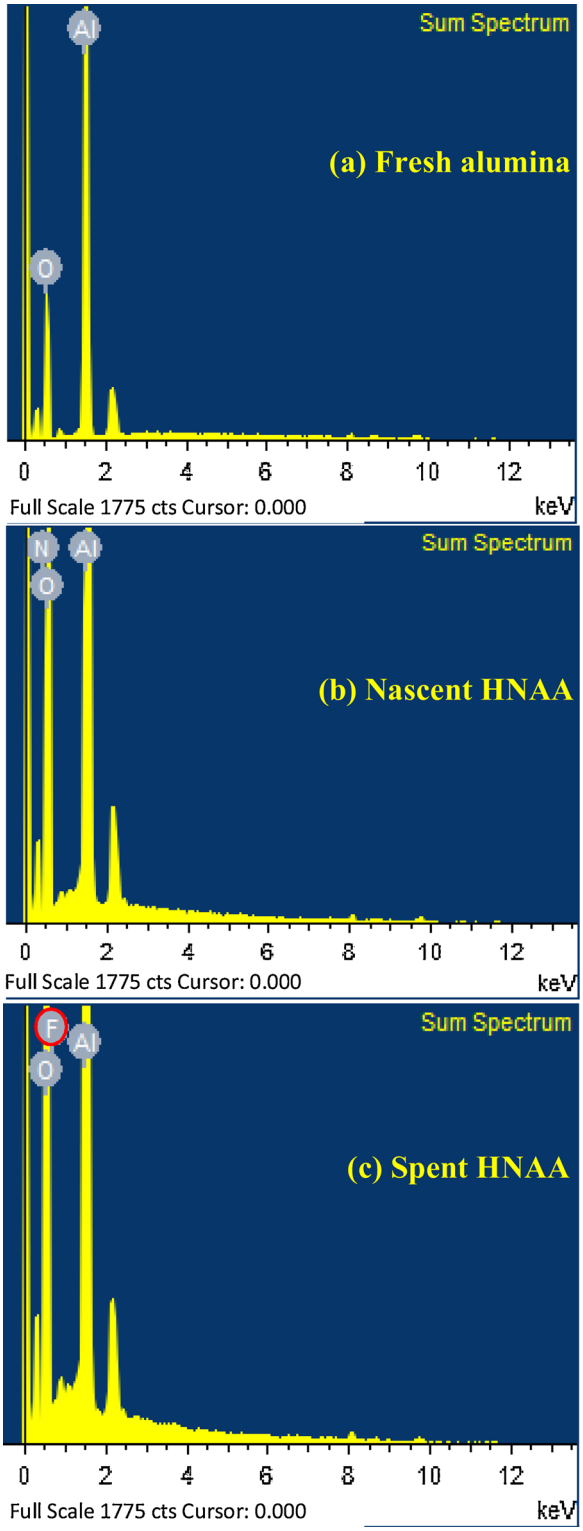

Fig. 3. EDX analysis of (a) fresh alumina (b) nascent HNAA adsorbent (c) spent HNAA adsorbent.

were conducted to analyze the change of physiochemical properties and stability of the adsorbent sample with the variation of temperature. The X-ray fluorescence (XRF) analysis of the alumina samples was carried out to examine the elemental and oxides wise composition (%).

The zero point charge (pH_{zpc}) of an adsorbent is that pH of the solution at which the net surface charge on the adsorbent is zero (i.e., electrically neutral). The pH drift method was applied for the estimation of pH_{zpc} of the adsorbent. The pH_{zpc} was determined by the point of interaction of lines pH_{final} = $pH_{initial}$ and pH_{final} as function of $pH_{initial}$ (Foo and Hameed, 2012; Sriprang et al., 2014).

The detail of instruments applied for the characterization of adsorbent samples is described in Supplementary Material.

2.6. Adsorption studies

The experiments were conducted to examine the influence of different parameters on adsorption of fluoride ions. The parameters considered for influencing the adsorption phenomena are initial pH (2–9), adsorbent dose (0 g/L-26 g/L), initial fluoride concentration (53 mg/L-449 mg/L), and impedance by the coexisting ions (SO_4^{2-}, HCO_3^-, Cl^-, CO_3^{2-}, NO_3^-). The operating temperature of 27 °C (except isotherm study) and stirring rate of 400 rpm were maintained to perform all the experiments. The pH and adsorbent dose were optimized (refer Supplementary Material for definition).

2.7. Adsorption isotherm

The adsorption experiments were performed at different temperatures (25 °C, 35 °C, and 45 °C) till equilibrium to investigate the effect of temperature on the removal of fluoride ions. The optimized condition of pH and adsorbent dose was maintained to conduct the study. The experimental data were attempted to fit into the non-linear curve fitting by Langmuir and Freundlich isotherm models. The Supplementary Material details the mathematical expression of Langmuir and Freundlich isotherm models (Wang et al., 2019a).

The separation factor (R_L) is another important parameter to evaluate the favorability of adsorbate adsorption. It is related to the Langmuir isotherm model. The mathematical expression of separation factor and its favorability criteria of adsorbate adsorption are depicted in Supplementary Material.

2.8. Adsorption kinetics

The kinetic study of fluoride ions adsorption was conducted at 20 mg/L, 40 mg/L, and 80 mg/L of fluoride concentration. The fluoride concentration was estimated at different time interval to obtain the rate of fluoride ions uptake by the adsorbent. The pseudo first and second order kinetic models were applied to explore the kinetics of fluoride ions adsorption on the adsorbent (Wang et al., 2019b). The expression of kinetic models is provided in Supplementary Material.

2.9. Thermodynamic study

The thermodynamic parameters essential to characterize the adsorption process are Gibbs free energy change (ΔG^o), enthalpy change (ΔH^o), and entropy change (ΔS^o). The method to estimate these parameters from their mathematical expressions is detailed in the Supplementary Material.

2.10. Effect of coexisting ions

The ground and industrial wastewater commonly contain the coexisting ions like bicarbonate, sulfate, chloride, carbonate and nitrate. These ions create hindrance in the adsorption of fluoride ions due to their electronegative nature. Therefore, it is essential to analyze the interference effect of these coexisting ions of wastewater. The study was performed at the 0.1 M concentration of coexisting ions.

2.11. Regeneration study

The regeneration study of the prepared adsorbent was examined by the application of sodium hydroxide. The study was initiated by preparation of spent adsorbent at initial fluoride concentration of 40 mg/L,

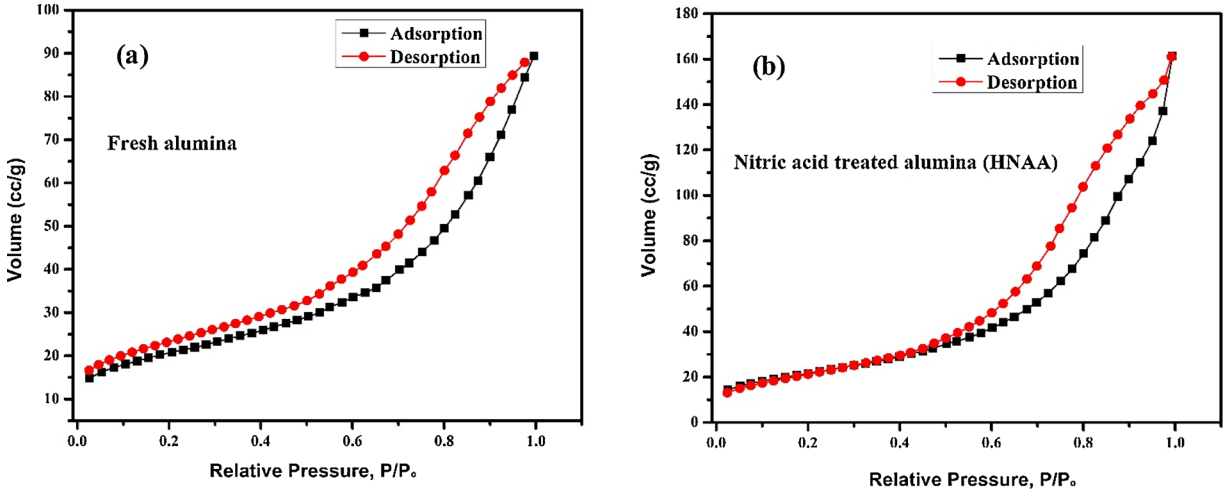

Fig. 4. N_2 adsorption-desorption isotherm plot of (a) fresh alumina (b) nitric acid treated alumina (HNAA) from BET analysis.

Table 1
BET and XRF analysis results of alumina before and after nitric acid treatment.

Materials	BET analysis			XRF analysis								
	S_{BET} (m^2/g)	V_{TOTAL} (cm^3/g)	D_{AVG} (Å)	Al (%)	O (%)	Fe (%)	Na (%)	S (%)	Si (%)	Mg (%)	Ca (%)	Others (%)
Fresh alumina	71.170	0.139	127.412	50.803	46.735	1.150	0.539	0.324	0.275	0.069	0.048	0.057
HNAA	78.691	0.249	106.790	51.379	46.878	0.879	0.145	0.368	0.197	0.060	0.021	0.073

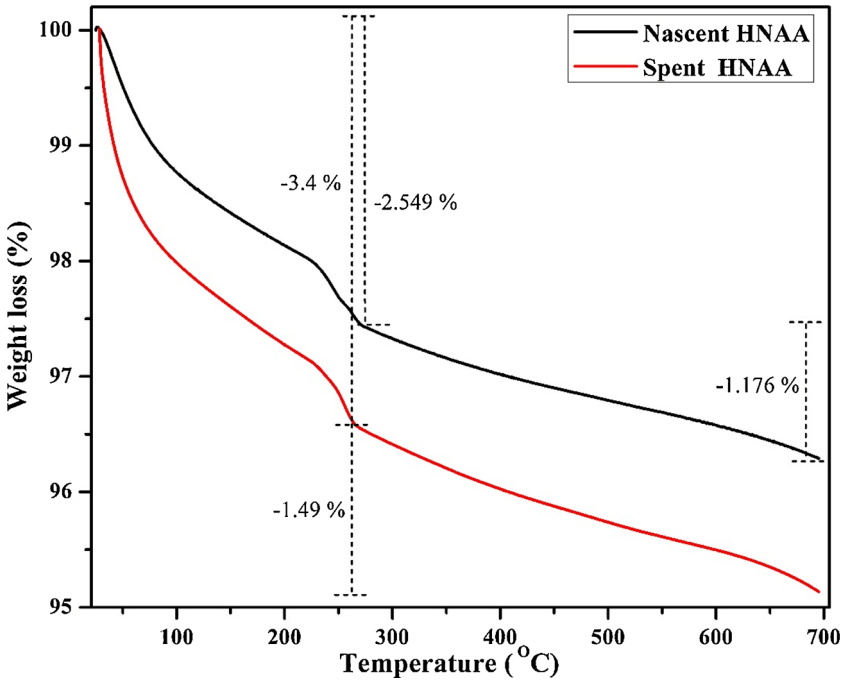

Fig. 5. TGA analysis of nascent and spent HNAA adsorbent.

adsorbent dose of 20 g/L, initial pH of 3.5, stirring rate of 400 rpm, contact time of 3 h, and operating temperature of 300 K. The spent adsorbent was dried (105 °C) in hot air oven. The dried spent adsorbent was treated with 0–3 M concentration of NaOH for the time period of 17 h. The measurement of desorbed fluoride ions concentration in the solution was conducted after 17 h. The regeneration of adsorbent is dependent on the percentage of fluoride ions desorbed. The mathematical expression to calculate the desorption percentage is given in Supplementary Material.

2.12. Reusability test of adsorbent

An adsorbent is economical to implement if it demonstrates the property of reusability. The reusability study was initiated by the regeneration of spent adsorbent as described above (Section 2.11). The regenerated adsorbent was water washed 3–4 times and dried (105 °C). The dried sample (20 g) was treated with HNO_3 acid, similar to Section 2.2, for neutralization of the alkaline effect caused by sodium hydroxide solution and reactivation of HNAA adsorbent. The same process of

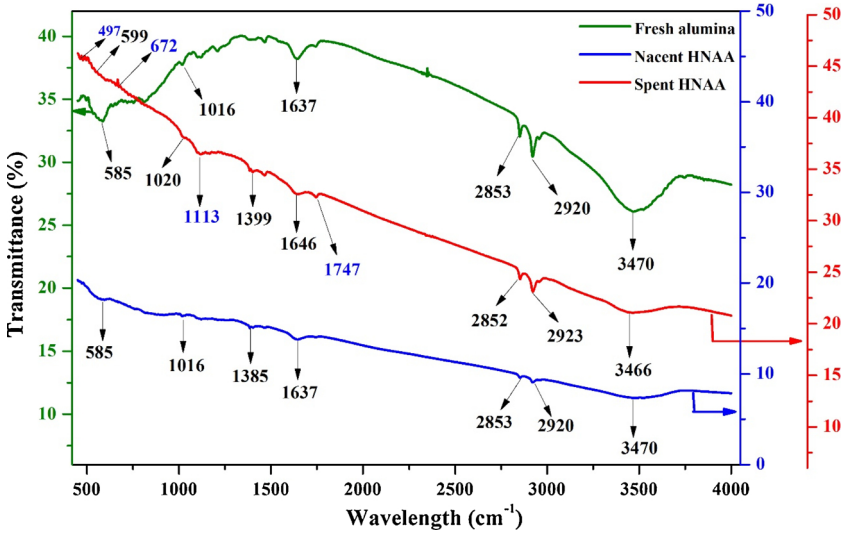

Fig. 6. FTIR spectrum of fresh alumina, nascent HNAA (before adsorption test) and spent HNAA (after adsorption test).

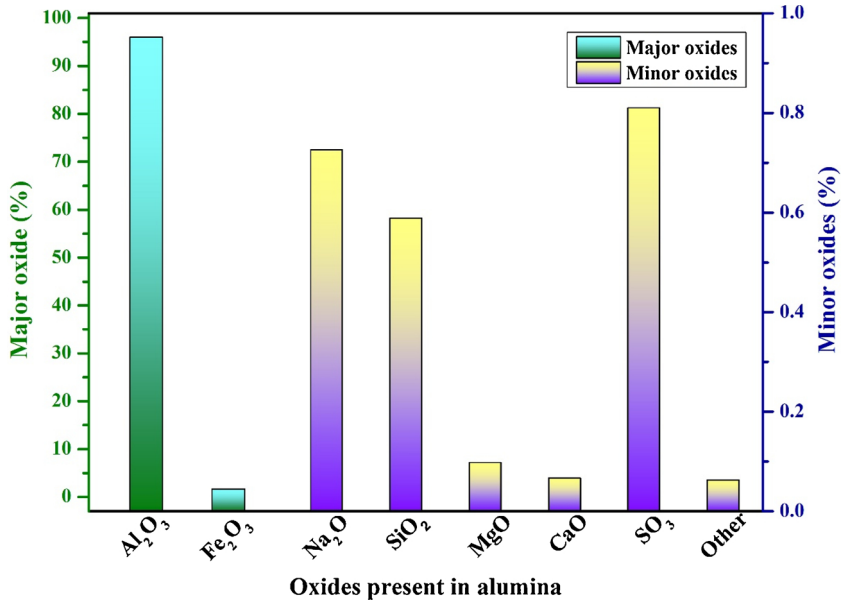

Fig. 7. XRF analysis of alumina.

regeneration, activation and adsorption was continued till significant drop in adsorption efficiency was noticed.

2.13. Effect of nitric acid treatment of alumina on fluoride removal

It is important to evaluate the effect of nitric acid activation of alumina on fluoride removal efficiency and adsorption capacity. The defluoridation experiments were performed by taking the fresh alumina and nascent HNAA. The parameters kept constant for the fluoride removal (%) experimentation were initial fluoride concentration of 40 mg/L, adsorbent dose of 20 g/L, initial pH of 3.5, stirring rate of 400 rpm, contact time of 3 h and 300 K operating temperature. In order to compare the performance of fresh alumina and nascent HNAA, in terms of the maximum adsorption capacity (Q_m), the isotherm study for both the alumina samples were conducted at the same operating condition.

2.14. Comparative performance of nitric and hydrochloric acid treated alumina

As mentioned earlier that Wu et al., (2010) have explored the HCl acid activated alumina for defluoridation in batch scale (Chen et al., 2010a). Therefore, the comparison of fluoride removal potential of HCl and HNO_3 acid treated alumina was investigated.

2.15. Application of HNAA on industrial wastewater

The defluoridation efficiency of prepared HNAA adsorbent was examined on industrial wastewater. The industrial wastewater for experimental purpose was provided by the aluminum industry of Odisha, India. The experiment was performed by similar procedure as described in Section 2.4. The wastewater characteristics were analyzed before (feed) and after (filtrate) equilibrium adsorption. The parameters considered for characterization were presence of ions, TDS (total dissolve solid), TOC (total organic carbon), conductivity and visible color. The description of instruments utilized for the characterization of industrial wastewater is provided in Supplementary Material.

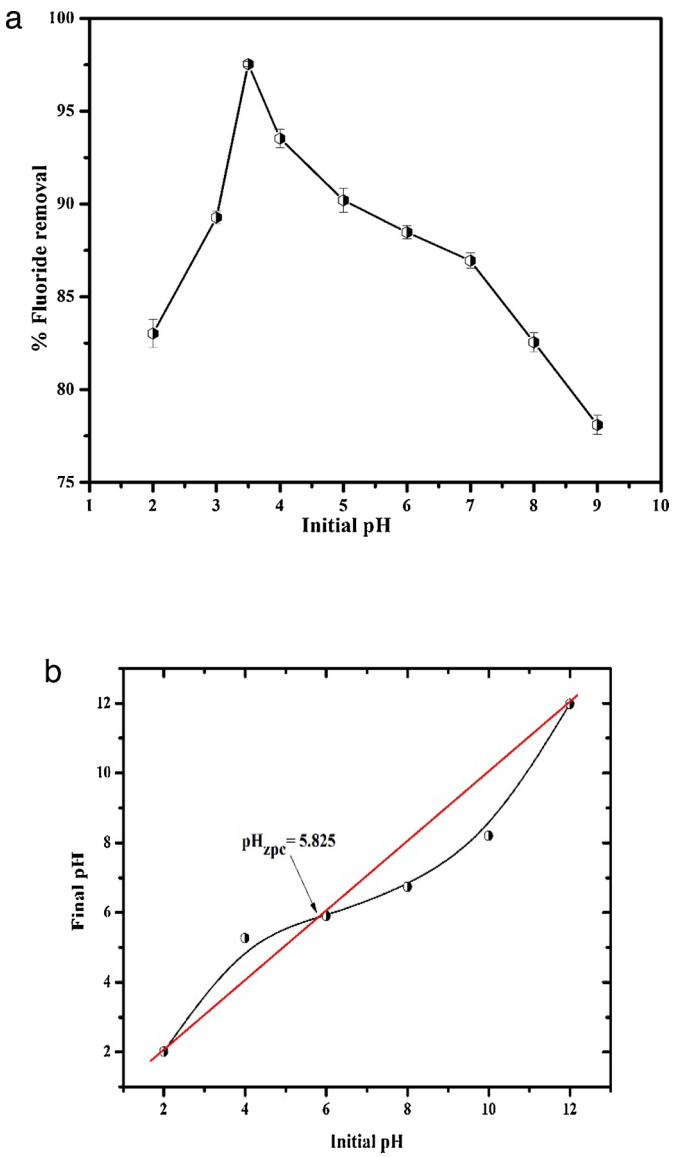

Fig. 8. (a) Effect of initial pH on removal of fluoride (b) Point of zero charge (pH_{zpc}) of HNAA adsorbent.

3. Results and discussion

3.1. SEM/EDX analysis

The surface texture of fresh alumina, nascent HNAA and fluoride adsorbed HNAA obtained from SEM analysis is represented in Fig. 2. It shows that the surface texture of fresh alumina is compact and non-porous (Fig. 2a). Whereas, the treatment of fresh alumina with nitric acid has imparted breakdown of its crystal structure. It results in imparting two types of surface morphology to HNAA: (i) disintegration of alumina crystallinity (Fig. 2b), and (ii) uniform opening of pores and cracks on the surface of alumina (Fig. 2c). It may have resulted in the enhancement of porous nature to fresh alumina. These alterations in the surface texture of alumina possibly has occurred due to the oxidizing nature of nitric acid. It adds up in the formation of additional surface area to fresh alumina. Therefore, it can be asserted that nitric acid treatment of fresh alumina enriches the additional pores or active surfaces for adsorption of fluoride ions. However, the fluoride adsorbed or spent HNAA shows depleted pores and filled gap texture on its surface (Fig. 2d). The surface of spent HNAA also shows coarsened texture compared to nascent HNAA. Both of these changes acquired by the spent HNAA may be due to the fixation of fluoride ions on the exposed surface of nascent HNAA.

The EDX analysis results of fresh alumina, nascent and spent HNAA are demonstrated in the Fig. 3. The fresh alumina shows the peak of aluminum and oxygen (Fig. 3a). Whereas, the additional peak of nitrogen is observed in nascent HNAA (Fig. 3b). It may be due to the existence of nitrate ions (NO_3^-) traces in the alumina which are not removed after water wash of HNAA. The successful adsorption of fluoride ions on nascent HNAA is asserted by the peak of fluoride in spent HNAA (Fig. 3c). The peaks of fluoride (F), oxygen (O), and nitrogen (N) appears to be closely located in the EDX spectrum (Fig. 3). The reason for the emergence of closely located peaks of F, O, and N is due to approximately close values of Kα (i.e., X-rays emission given off when electron return to the K electron shell) for these elements. The Kα values of N, O, and F are 0.2774, 0.3924, and 0.5249, respectively. It asserts the level of closeness of X-ray emission peaks.

3.2. BET analysis

To understand the nature of pores generated because of nitric acid activation of alumina, BET analysis was carried out. The N_2 adsorption-desorption isotherm plots of fresh alumina and nascent HNAA adsorbent obtained from BET analysis are shown in Fig. 4. The nature of isotherm curve for both the samples is found to follow the parallel trend. The difference noticed in the pattern of N_2 adsorption-desorption isotherm curves of fresh alumina and nascent HNAA is possibly due to the nitric acid treatment of fresh alumina. Considering the plot of nascent HNAA, as per the IUPAC standard, the nature of N_2 adsorption-desorption isotherm plot resembles with type IV isotherm (Lin et al., 2006). It implies the mesoporous nature of nascent HNAA. Besides, the pattern of the isotherm curve of nascent HNAA indicates the narrow slit-shaped pores (Lin et al., 2006). The results of specific surface area (S_{BET}), total pore volume (V_{TOTAL}), and average pore diameter (D_{AVG}) of fresh alumina and nascent HNAA are represented in Table 1. The error in the measurement of BET analysis results is 5%. Table 1 demonstrates that S_{BET} and V_{TOTAL} of alumina particles is increased after treatment with nitric acid. This is expected to enhance the adsorption capacity of fresh alumina (Siswoyo et al., 2019). The increased S_{BET} confirms the opening of additional pores in fresh alumina. It is due to the oxidizing nature of nitric acid which imparts the breakdown and disintegration of crystallinity of alumina. The SEM analysis has also given the alike results. Besides, the DFT result of BET analysis is demonstrated in Fig.S1. It represents that most of the surface area of HNAA is due to pore width up to 255 Å.

3.3. TGA analysis

The TGA analysis result of HNAA adsorbent before and after fluoride adsorption is provided in Fig. 5. It depicts that the overall weight loss of nascent and spent HNAA, in the analysis temperature range of 27 °C–700 °C, is 3.725% and 4.89%, respectively. The nascent HNAA shows the weight loss (%) in two regions. In the first region (i.e., 25 °C–270 °C), the weight loss of 3.4% is observed. It is may be due to loss of moisture and hydroxyl groups present on alumina. In the second region (i.e., 270 °C–700 °C), the steady weight loss of 1.49% can be observed. It is possibly due to the steady thermal degradation of alumina particles at high temperature. Similar result of TGA analysis was described by other researcher too (Wu et al., 2017). The weight loss pattern for spent HNAA is found to be similar to that of nascent HNAA.

3.4. FTIR analysis

The FTIR spectra of fresh alumina, nascent HNAA and spent HNAA can be seen from Fig. 6. The nitric acid treatment of fresh alumina has imparted two changes in the FTIR spectrum: (i) decreased percent transmittance of nascent HNAA (ii) alteration in the intensity of few

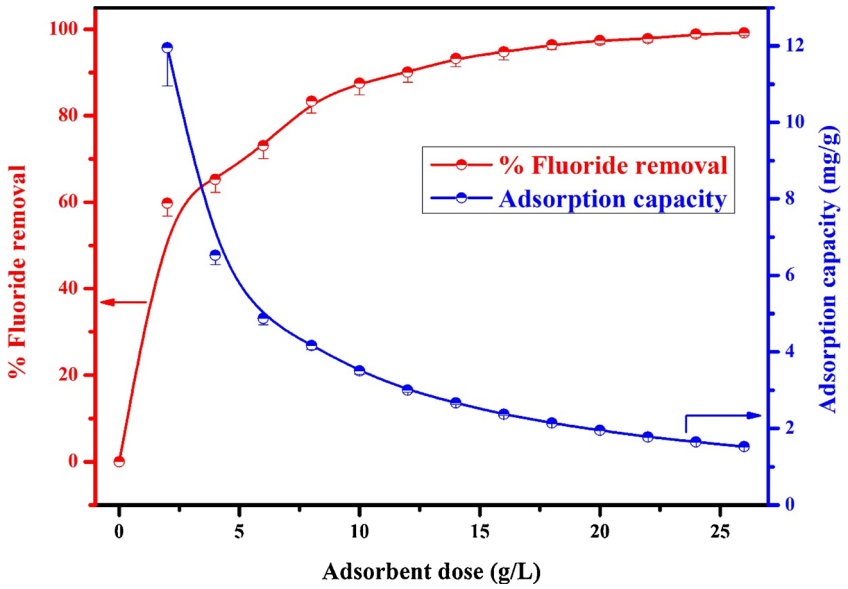

Fig. 9. Effect of adsorbent dose on removal of fluoride (experimental operating condition- pH: 3.5, fluoride concentration: 40 mg/L, Temperature: 300 K, time: 3 h and stirring rate: 400 rpm).

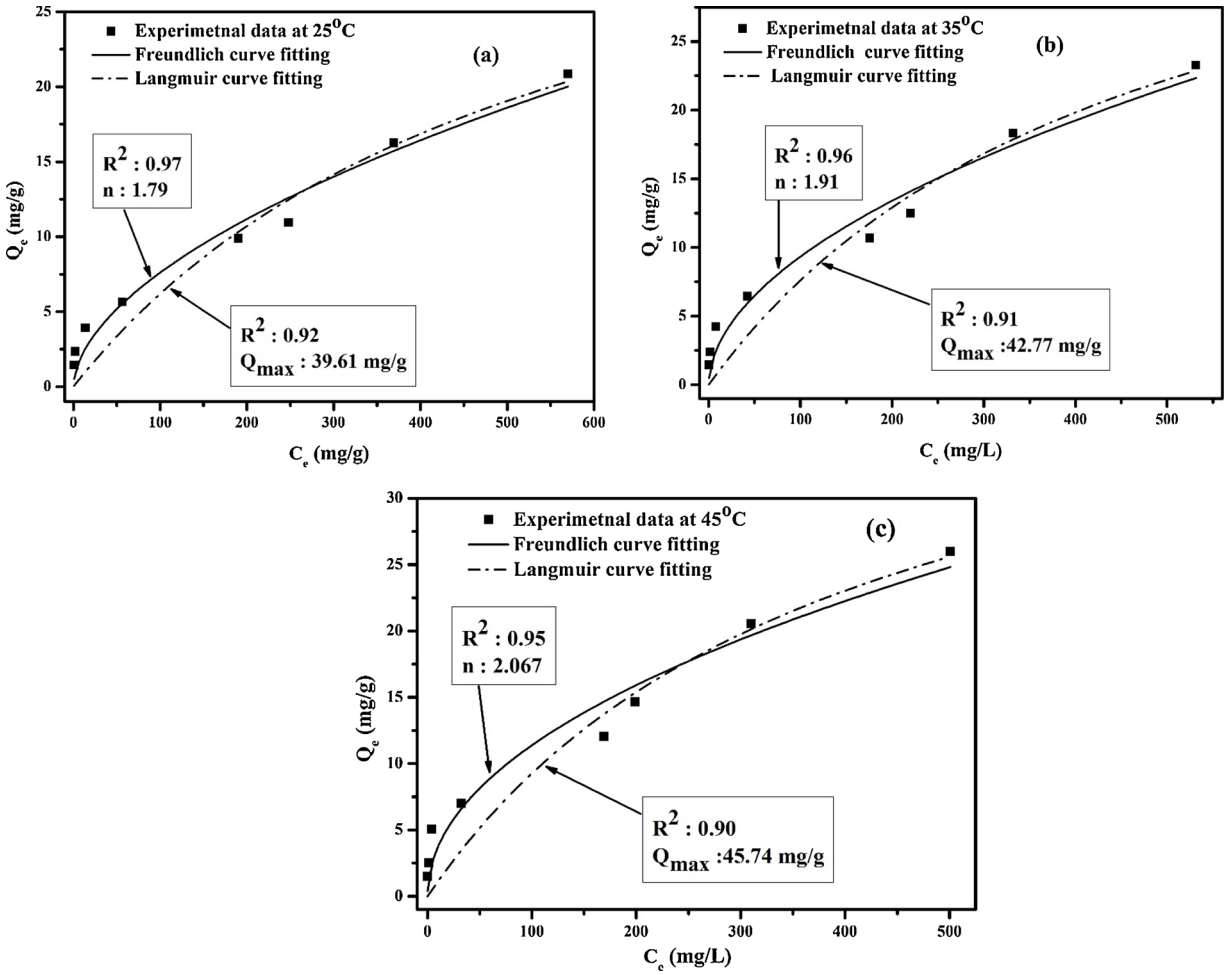

Fig. 10. Isotherms of fluoride adsorption on HNAA at (a) 25 °C (b) 35 °C, and (c) 45 °C (operating condition: pH of 3.5, adsorbent dose of 20 g/L, and stirring rate of 400 rpm).

Table 2
Langmuir and Freundlich isotherm constants at 25 °C, 35 °C, and 45 °C temperature.

Temperature (K)	Langmuir constants			Freundlich constants		
	K_L(L/mg)	Q_m(mg/g)	R^2	K_f ($mg^{1-1/n}$ $L^{1/n}$ g^{-1})	n	R^2
298	0.00150	39.609	0.924	0.5876	1.7986	0.966
308	0.00287	42.777	0.915	0.8389	1.9121	0.963
318	0.00424	45.749	0.904	1.2279	2.0679	0.957

Table 3
Fluoride adsorption capacity comparison of HNAA with other adsorbents.

Adsorbents	Max adsorption capacity (mg/g)	References
Nano alumina	14.0	(Kumar et al., 2011)
Activated alumina (Grade OA-25)	0.74	(Ghorayi and Pant, 2004)
Activated alumina	16.30	(Ku and Chiou, 2002)
Mesoporous ϒ-alumina	3.48	(Dayananda et al., 2015)
Granular ceramic	12.12	(Chen et al., 2010b)
Metallurgical grade alumina	12.21	(Pietrelli, 2005)
2D-Al_2O_3	41.30	(Huang et al., 2016)
Al_2O_3-ZrO_2 binary adsorbent	114.54	(Zhua et al., 2015)
Fe-Al-Ce trioxide adsorbent	178.0	(Wu et al., 2007)
HNAA	45.75	Present work

peaks. Considering the spectrum of nascent HNAA, the peak located at 3470 cm^{-1} indicates O—H stretching vibration arising from water molecules (Ma et al., 2017; Adak et al., 2017). The adsorption band in between 2500 cm^{-1} and 3000 cm^{-1} is due to —OH stretching vibration (Lu et al., 2013). The 1637 cm^{-1} peak on nascent HNAA assigned to bending vibration of the O—H group (Hussain et al., 2015). The Al-O linkage is indicated by the peak at 1016 cm^{-1}. The peaks in the range of 400-1000 cm^{-1} signify the Al—O and Al—OH vibration frequency (Hussain et al., 2015; Costa et al., 1999). The adsorption band present on nascent HNAA at 1385 cm^{-1} is characteristics for NO_3^- ions (Abou et al., 2008). The presence of peak for nitrate ions is possibly due to unremoved traces of nitric acid from nascent HNAA. However, post fluoride adsorption two types of changes are observed in the FTIR spectrum: (i) increased percent transmittance of spent HNAA (ii) shift in the location of peaks. The peaks of FTIR spectrum located at 3470 cm^{-1}, 2920 cm^{-1}, 2853 cm^{-1}, 1637 cm^{-1}, 1016 cm^{-1}, and 585 cm^{-1} are shifted to 3466 cm^{-1}, 2923 cm^{-1}, 2852 cm^{-1}, 1646 cm^{-1}, 1020 cm^{-1}, and 599 cm^{-1}, respectively. It is possibly due to adsorption of fluoride ions on nascent HNAA adsorbent by ion exchange with hydroxyl ions. The same size and isoelectric property of hydroxyl and fluoride ion facilitates the ion exchange between both the ions (Layden et al., 1980). The shift in the peak of 1385 cm^{-1} to 1399 cm^{-1} is possibly due to ion exchange of nitrate ions with the fluoride ion. In addition, several new peaks on the spectrum of spent HNAA are found to be emerge at 1747 cm^{-1}, 1113 cm^{-1}, 672 cm^{-1}, and 497 cm^{-1}. As metal oxides (e.g. alumina) are known for their electropositive nature. Therefore, emergence of these new peaks is possibly due to electrostatic attraction between electronegative fluoride ions and electropositive aluminum metal present in alumina. Hence, this study concludes that the ion exchange and electrostatic attraction mechanism of fluoride adsorption contribute to the adsorption of fluoride ions on the nascent HNAA.

3.5. XRF analysis

The Fig. 7 shows the XRF analysis result of alumina sample in oxides form. It reveals that the major oxides (wt% > 1) of alumina are Al_2O_3 and Fe_2O_3. Whereas, the minor oxides (wt% < 1) of alumina are MgO, SiO_2, SO_3, Na_2O, CaO and other as impurities.

On the other hand, the elemental composition of fresh alumina before and after acid treatment is provided in Table 1. It shows that the percent composition of the elements like iron, sodium, silica, magnesium and calcium has reduced after nitric acid treatment. It may be due to the formation of nitrates of these elements after acid treatment of fresh alumina. These nitrates possibly get removed after multiple water wash of nitric acid treated alumina.

3.6. Effect of initial pH of wastewater

The initial pH of wastewater modifies the surface property of adsorbent which in turn results in major influence on fluoride ions adsorption from the wastewater (Wang et al., 2017a; Siswoyo et al., 2014; Siswoyo and Tanaka, 2013). The experimental result of initial pH effect on the removal of fluoride ions is demonstrated in Fig. 8(a). It shows that the fluoride removal efficiency of the adsorbent is increased with the increase of adsorbate pH from 2 to 3.5. But, with the increase of pH from 3.5 to 9, the decrease in the fluoride removal efficiency is observed. This dependency trend of percent fluoride removal on initial pH is attempted to explore by pH_{zpc} of HNAA adsorbent. The pH_{zpc} of HNAA is found at 5.825 (Fig. 8b). It reveals the electropositive nature of HNAA adsorbent surface in the solution pH < pH_{zpc}. Therefore, the more electronegative fluoride ions should be attracted toward the electropositive surface of the HNAA adsorbent at low pH. However, the result obtained in the acidic region is the reduction of defluoridation (%). The low pH of wastewater favors the existence of weak acid HF and the electropositive complex like AlF^{2+} and AlF^{+} (Clifford et al., 1978). Hence, the adsorption of fluoride ion is reduced at the low pH < pH_{zpc}.

On the other hand, at the high pH > pH_{zpc}, the surface of adsorbent is electronegative causing the electrostatic repulsion between adsorbent surface and electronegative fluoride ions. Therefore, the adsorption of fluoride ion is reduced at higher pH.

Both of these opposing factors possibly impart negligible hindrance at pH of 3.5 which contribute to the maximum removal of fluoride ions. Hence, the pH of 3.5 is considered as optimum one for all the experiments.

The Fig. 8a shows that fluoride removal is considerably high (nearly 86%) up to pH of 7. The reason of nearly 86% of defluoridation is possibly due to partial deprotonation from the adsorbent surface (refer Supplementary Material for significance of pH_{zpc} in protonation/deprotonation). The presence of partial protonated surface of adsorbent possibly has imparted electrostatic attraction of F^- ions resulting in nearly 86% fluoride removal.

3.7. Effect of adsorbent dose

The adsorbent dose is another influencing factor for adsorption of adsorbate on the surface of adsorbent. The effect of HNAA adsorbent dose on adsorption of fluoride ions is demonstrated in Fig. 9. It shows that removal of fluoride ions rises sharply with the increase of adsorbent dose from 0 to 8 g/L. Further increment in the adsorbent dose from 10 to 26 g/L gradually leads to the attainment of saturation in fluoride removal (%).

The profile of percent fluoride removal versus adsorbent dose is explained by the variation in the number of active adsorption sites with the change of adsorbent dose (Fig. 9). As the ratio of fresh alumina (g) and nitric acid (mL) taken for preparation of HNAA adsorbent was fixed (i.e., 1:1) (Section 2.2). Therefore, the number of active sites created on unit amount alumina can be considered constant. Hence, the low adsorbent dose provides the less number of active sites for fluoride ion adsorption, resulting in lowering the efficiency of fluoride removal (%). But, the increase of adsorbent dose facilitates the enhanced number of active sites for adsorption of fluoride ions. It results in the increment of

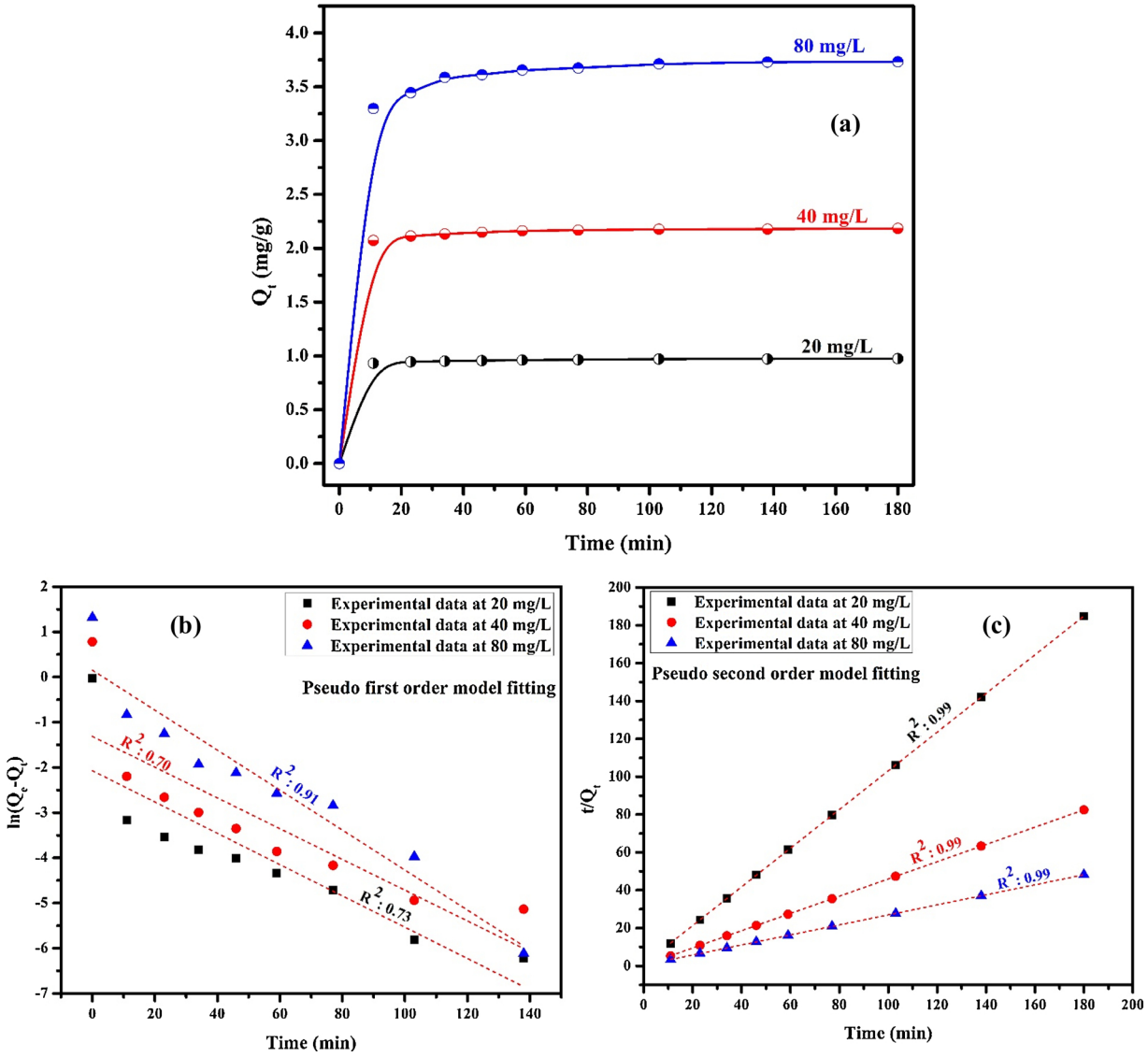

Fig. 11. Effect of contact time (a) experimental data at 20 mg/L, 40 mg/L, and 80 mg/L fluoride concentration (b) Pseudo first order model fitting (c) Pseudo second order model fitting (operating condition: pH: 3.5, adsorbent dose: 20 g/L, Temp.: 300 K, stirring rate: 400 rpm).

Table 4
Parameters of pseudo first and second order kinetics model.

Kinetic model	Initial fluoride concentration (mg/L)			
	20	40	80	
$Q_{e\ (experimental)}$, mg/g	0.974	2.183		3.732
Pseudo first order				
R^2	0.727	0.703		0.915
k_1 (min^{-1})	0.044	0.034		0.035
$Q_{e\ (calculated)}$, mg/g	0.126	0.269		1.166
Pseudo second order				
R^2	0.999	0.999		0.999
k_2 (g/mg)	1.170	0.544		0.140
$Q_{e\ (calculated)}$, mg/g	0.978	2.192		3.775

Table 5
Evaluation of thermodynamics parameters.

ΔH^o (kJ/mol)	ΔS^o (kJ/mol K)	ΔG^o (kJ/mol)			R^2
		298 K	308 K	318 K	
40.81	0.165	−8.301	−10.246	−11.604	0.97

percent fluoride removal. The saturation of fluoride removal efficiency, at 24 g/L-26 g/L, is due to the removal of almost all the fluoride ions. The profile of drop in fluoride concentration can be justified by similar reasons (Fig.S2). The variation of fluoride adsorption capacity is found to be just opposite to the variation of percent fluoride removal. The increase of adsorbent dose causes the availability of unutilized active sites due to the fixed amount of fluoride concentration (i.e., 40 mg/L) taken. Therefore, at high adsorbent dose, the presence of abundant number active sites which are not captured by fluoride ions results in reduction of adsorption capacity. The Fig.S2 indicates that the adsorbent dosage of 20 g/L is requisite to drop the fluoride ions concentration from 40 mg/L to 1.025 mg/L (i.e., < 1.5 mg/L). Therefore, the 20 g/L of adsorbent dose is considered as the optimum dose for all the experiments.

The effect of initial fluoride concentration on fluoride removal (%) by HNAA absorbent is shown in Fig.S3. It demonstrates that the rise of initial fluoride concentration results in gradual decrease in fluoride removal (%) and it finally leads to saturation stage. The possible cause of this variation is gradual decrease in the number active sites of HNAA due to fixation of more fluoride ions with the increase of fluoride

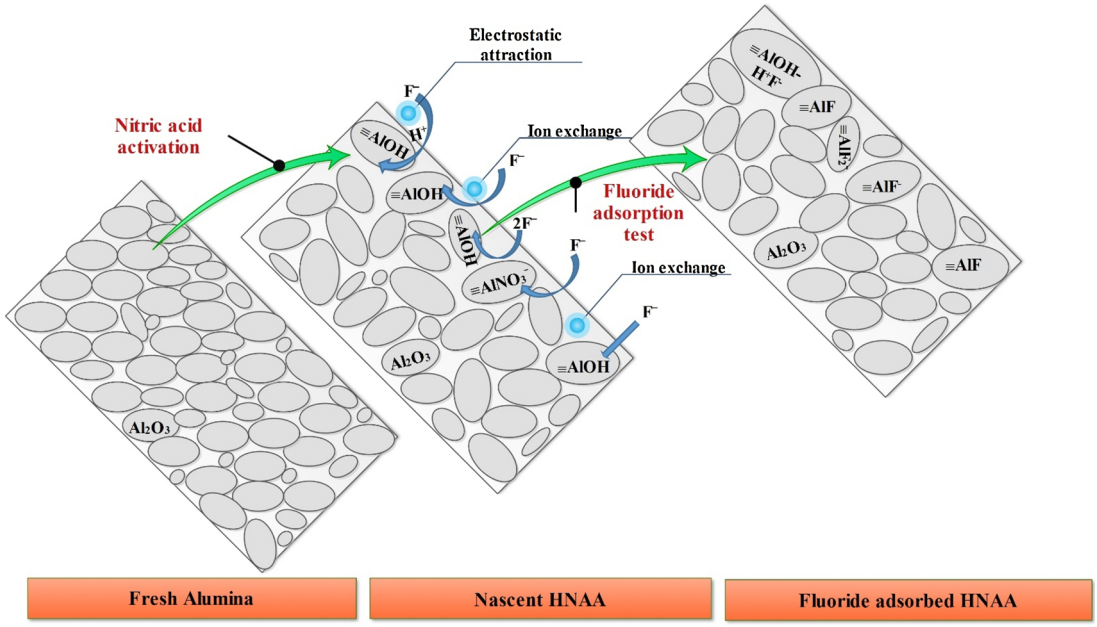

Fig. 12. Mechanism of fluoride ion adsorption.

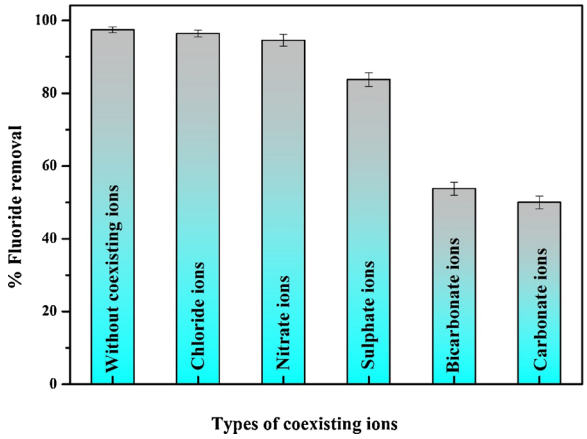

Fig. 13. Effect of coexisting ions on removal of fluoride (operating condition - fluoride concentration: 40 mg/L, pH: 3.5, adsorbent dose: 20 g/L, temp.: 300 K, stirring: 400 rpm, coexisting ions concentration: 0.1 M).

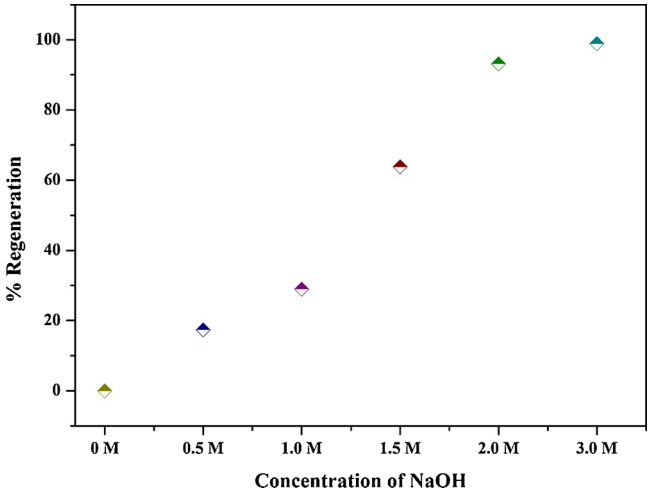

Fig. 14. Regeneration of NHAA by sodium hydroxide.

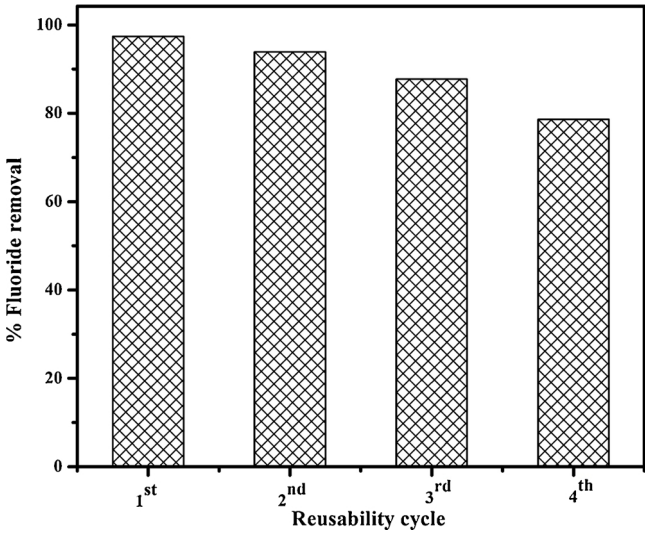

Fig. 15. Reusability study of HNAA adsorbent.

concentration. At very high fluoride concentration (i.e. 360 mg/L to 449 mg/L) the occupancy of almost all the active sites may be ascribed to saturation in percent fluoride removal.

3.8. Isotherm study

The adsorption isotherm study depicts the nature of adsorbate affinity to the adsorbent. It is also helpful to understand the mechanism of adsorption, behavior of adsorbent surface, affinity and favorability of adsorbate to adsorbent surface. The isotherm study reveals the extent up to which the adsorbate is acquired by the adsorbent (Q_e) and extent of adsorbate retained by the solution (C_e) (Lima et al., 2015). Here, we report the Langmuir and Freundlich isotherm models to explore the nature of fluoride ions adsorption on HNAA adsorbent (Lima et al., 2015).

For the estimation of maximum adsorption capacity (Q_m) of the adsorbent, it is essential that equilibrium adsorption capacity (Q_e) value should outstretch up to the plateau region (Tien, 1994). Therefore, the concentration of fluoride ions in synthetic wastewater was varied up to

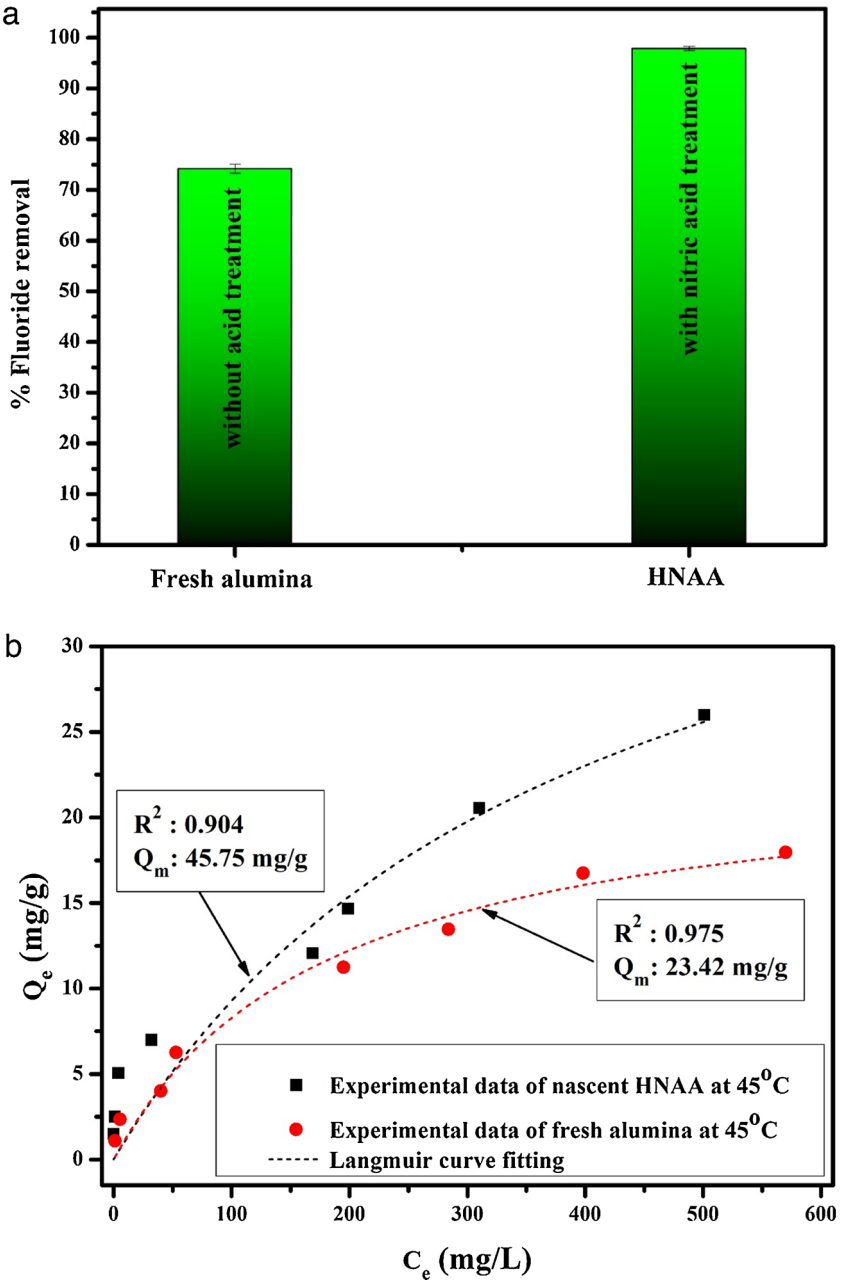

Fig. 16. (a) Fluoride removal efficiency of alumina before and after nitric acid treatment (operating condition: pH: 3.5, adsorbent dose: 20 g/L, fluoride concentration: 40 mg/L, Temp.: 300 K, stirring: 400 rpm), (b) Maximum adsorption capacity of alumina before and after nitric acid treatment (operating condition - pH: 3.5, adsorbent dose: 20 g/L, temperature: 45 °C, stirring rate: 400 rpm).

Table 6
Comparison of acid treatment of alumina by HNO_3 and HCl acid.

Acid applied for treatment of alumina	Wastewater tested	Operating condition for synthetic wastewater treatment				Equilibrium adsorption time	Q_{max} (mg/g)	Ref.
		pH	dose (g/L)	Initial fluoride concentration (mg/L)	Percent removal efficiency			
HCl	Synthetic	7	5	23.27	8.37%	50 h	NA*	(Chen et al., 2010a)
HNO_3	Synthetic and industrial	3.5	20	40	97.43%	3 h	45.75	Present work

*Not available.

964 mg/L, for the isotherm study.

The Fig. 10 shows the profile of experimental data and non-linear curve fitting by Langmuir and Freundlich isotherm models. The parameters of the non-linear curve fitting are provided in Table 2. It indicates the higher values of R^2 (correlation coefficient) for Freundlich isotherm model than Langmuir isotherm model, at all temperature.

Table 7
Industrial wastewater characteristics before and after treatment with HNAA.

Wastewater	F^- (mg/L)	Cl^- (mg/L)	Br^- (mg/L)	NO_3^- (mg/L)	Ca^{2+} (mg/L)	Mg^{2+} (mg/L)	Fe^{2+} (mg/L)	TOC (mg/L)	TDS (10^{-6} ×mg/L)	Conductivity (10^{-4} ×S/m)	Color
Feed*	17.5	6179.53	4.4306	13.243	403.33	33.872	0.177	21.935	8.293	10.957	Yellowish
Filtrate**	0.845	3422.25	1.169	9.256	275.05	15.935	0.0241	9.87	5.477	8.84	Transparent

*Before adsorbent treatment; **After adsorbent treatment.

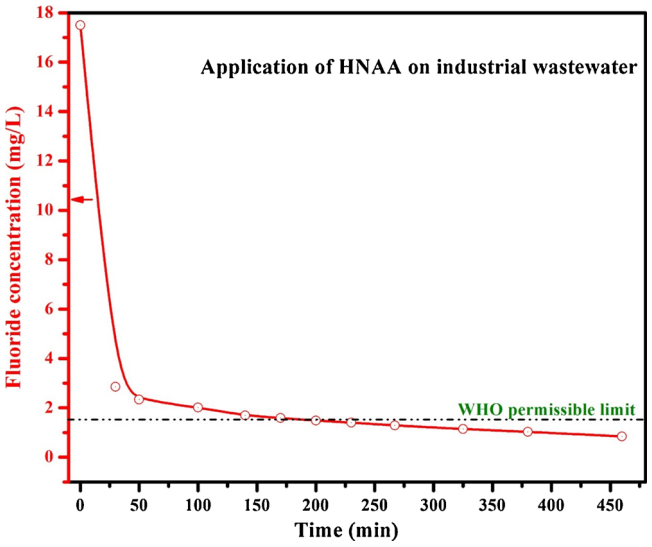

Fig. 17. Defluoridation testing of industrial wastewater (operating condition - adsorbent dose: 20 g/L, stirring: 400 rpm, temperature: 300 K).

Hence, the adsorption of fluoride ions on HNAA can be concluded to be better fitted by Freundlich isotherm model than that of Langmuir isotherm model. Therefore, it can be asserted that the dominant mechanism of fluoride adsorption on the adsorbent is heterogeneous adsorption (Lima et al., 2015). The maximum adsorption capacity (Q_m) exhibited by HNAA adsorbent is 45.749 mg/g at 45 °C (Table 2). The Q_m of adsorbent is found to increase with the rise of temperature. It implies the endothermic nature of fluoride adsorption on HNAA adsorbent (Lima et al., 2015). The favorability of fluoride ions adsorption is asserted by the value of $n > 1$ and $K_L > 0$. The Fig.S4 represents the variation of separation factor (R_L) in the range of $1 > R_L > 0$. It re-asserts the favorability of fluoride adsorption on the adsorbent.

The Q_m of HNAA obtained from the Langmuir isotherm curve fitting is compared with the other alumina based adsorbents mentioned in the literature (Table 3) (Kumar et al., 2011; Ghorayi and Pant, 2004; Ku and Chiou, 2002; Dayananda et al., 2015; Chen et al., 2010b; Pietrelli, 2005; Huang et al., 2016; Zhua et al., 2015; Wu et al., 2007). It shows that the maximum fluoride adsorption capacity of HNAA is comparable among the listed adsorbents. It also signifies the potential applicability of the HNAA adsorbent. The HNAA adsorbent, however, represents the low Q_m compared to the few adsorbents listed in Table 3. The attempt is being made to further enhance the adsorption capacity of HNAA adsorbent.

3.9. Kinetic study

The kinetics of the adsorption process is controlled by different parameters like structural characteristics of adsorbent, concentration and properties of adsorbate, and nature of adsorbate-adsorbent interaction (Nie et al., 2012b). The kinetic study is performed to obtain the profile of adsorbate concentration in aqueous solution of adsorbate and adsorbent. It is also helpful to obtain the rate of fluoride ion uptake by the adsorbent for estimation of the equilibrium time of adsorption, and mechanism of adsorbate adsorption.

The experimental data of kinetic study and linear curve fitting by pseudo first and second order kinetic models are represented in Fig. 11. The fitting parameters of the experimental data are provided in Table 4. It can be noticed from Fig. 11(a) that adsorption of fluoride ions by HNAA is very fast in the initial time period and later it becomes steady. The equilibrium adsorption of fluoride is reached in the contact time of 3 h. Table 4 and Fig. 11(b–c) depicts that R^2 of pseudo second order kinetic model is higher than the pseudo first order kinetic model at all concentration of fluoride. Besides, the $Q_{e\ (experimental)}$ values show the close match with $Q_{e\ (calculated)}$ values for pseudo second order kinetic model (Table 4). Therefore, the fluoride ions adsorption on HNAA can be stated to be dominated by the pseudo second order kinetic model. It signifies the chemisorption where the rate limiting step is associated with the valency forces through sharing or exchange of electrons (Aly et al., 2014).

3.10. Thermodynamics study

The thermodynamic parameters like ΔG^o, ΔH^o, and ΔS^o are helpful in understanding the mechanism of adsorption and nature of the isolated system of adsorbate and adsorbent. The adsorption is classified into physisorption and chemisorption depending on $\Delta H^o < 40$ kJ/mol and $\Delta H^o > 40$ kJ/mol, respectively (Liu et al., 2016). Table 5 represents the parameters of thermodynamic study.

The spontaneous and feasible nature of fluoride ions adsorption on the HNAA adsorbent can be confirmed by the negative values of ΔG^o. The more favorability of fluoride ions adsorption at higher temperature is exhibited by higher negative values of ΔG^o (Liu et al., 2016). The endothermic nature of fluoride ions adsorption on HNAA is revealed by the positive ΔH^o. Besides, the magnitude of $\Delta H^o > 40$ kJ/mol also asserts the chemisorption of fluoride ions on HNAA. Moreover, the positive ΔS^o suggests about the increase of randomness of fluoride species at the adsorbate-adsorbent interface during adsorption of fluoride ion on HNAA surface (Fu et al., 2015).

3.11. Mechanism of fluoride adsorption on the HNAA adsorbent

The mechanism of fluoride ions adsorption on HNAA adsorbent is predicted on the basis of characterization (i.e., EDX and FTIR) and experimental results. The FTIR result implied the existence of hydroxyl ions and its involvement in adsorption of fluoride ions. Besides, the EDX and FTIR results also revealed the existence of nitrate ions on HNAA which is linked with fluoride ion adsorption. Therefore, the possible mechanism of fluoride ions adsorption on HNAA is given as follows (Wang et al., 2017b; Zhou et al., 2018),

(i) Electrostatic attraction: It is applicable in the acidic environment which facilitates the protonation on surface hydroxyl of nascent HNAA adsorbent (Eq. (2)). It results in making the adsorbent surface electropositive. This favors the adsorption of negatively charged fluoride ions on to the positively charged adsorbent surface by the electrostatic force of attraction.

$$\equiv A\text{-}OH + H_2O\text{-}H^+ + F^- \rightarrow \equiv A\text{-}OH\text{-}H^+\text{-}F^- + H_2O \quad (2)$$

(ii) Ion exchange: The functional groups (i.e., hydroxyl and nitrate)

attached to the surface of adsorbent facilitate in ion exchange with fluoride ions as follows,

$$\equiv A\text{-}OH + H_2O\text{-}H^+ + F^- \rightarrow \equiv A\text{-}F + 2H_2O \quad (3)$$

$$\equiv A\text{-}OH + 2F^- \rightarrow \equiv A\text{-}F_2^- + H_2O \quad (4)$$

$$\equiv A\text{-}NO_3^- + F^- \rightarrow \equiv A\text{-}F^- + NO_3^- \quad (5)$$

where, ≡A symbol represents the active adsorption site on HNAA adsorbent. The Eqs. (3) and (4) are demonstrated for the moderate and high concentration of fluoride ions, respectively, where F^- ions get exchanged with OH^- ions. The presence of nitrate ions on the surface of HNAA possibly get exchanged by fluoride ions as shown by Eq. (5). The whole mechanism of fluoride ions adsorption is briefly demonstrated in Fig. 12.

3.12. Effect of coexisting ions

The effect of coexisting ions on percent fluoride removal is demonstrated in Fig. 13. From Fig. 13, it can be observed that hindrance in the fluoride ion adsorption by co-existing ions is in the order of $Cl^- < NO_3^- < SO_4^{2-} < HCO_3^- < CO_3^{2-}$. The defluoridation of wastewater (40 mg/L) without coexisting ions is 97.44%. Whereas, the presence of coexisting ions like chloride, nitrate, sulfate, bicarbonate and carbonate have reduced the fluoride removal by 96.43%, 94.55%, 83.74%, 53.75%, and 50.01%, respectively. The reason of the above order of hindrance is because of alteration in pH of wastewater after incorporation of salt of coexisting ions. It is noticed that the initial pH of wastewater (i.e., 3.5) is altered to 3.65 ± 0.02, 3.80 ± 0.23, 4.67 ± 0.75, 8.24 ± 0.21, and 10.88 ± 0.33 after incorporation of salt of chloride, nitrate, sulfate, bicarbonate and carbonate, respectively. Therefore, the coexisting ions which are capable of altering the pH of the wastewater to the higher alkaline range have the higher impact on defluoridation compared to coexisting ions capable of shifting the pH to low pH range. The change in the pH of wastewater to the higher alkaline region may have created higher competition to fluoride ions to get adsorbed on the same active site of HNAA. Hence, the examination of coexisting ions is requisite before defluoridation of wastewater by the HNAA adsorbent.

3.13. Regeneration study of HNAA

The regeneration result of HNAA at different concentration of sodium hydroxide is shown in Fig. 14. It is found that higher molarity of NaOH concentration is favorable for desorption of higher concentration of fluoride ions. The percent regeneration of the HNAA rises gradually with the increase of NaOH molarity from 0 to 3 M. The Fig. 14 shows that the 2 M of NaOH is capable of 93.12% regeneration. Whereas, the 3 M NaOH results in 98.86% regeneration. Therefore, it can be asserted that the 3 M NaOH is capable of desorbing almost all the adsorbed fluoride ions from the spent adsorbent. It implies towards the reuse of HNAA adsorbent.

3.14. Reusability test of adsorbent

For reusability study, the regeneration of spent HNAA adsorbent was carried out at 3 M concentration of NaOH. The fluoride removal efficiency of HNAA is found to decrease gradually and it reaches to 78.65% after four cycles of reusability (Fig. 15). The decrease in the performance of HNAA with the increase of reusability cycles is possibly due to: (i) blockage of active sites of adsorbent (ii) the loss of adsorbent material due multiple water wash during repetition of experiments.

3.15. Effect of nitric acid treatment of alumina on fluoride ions adsorption

The effect of nitric acid treatment of alumina on fluoride removal efficiency and adsorption capacity is shown in Fig. 16. It shows that the fluoride removal efficiency of alumina is enhanced from 74.18% to 97.43% after nitric acid treatment (Fig. 16a). On the other hand, the Q_m (maximum adsorption capacity) of HNAA was found to be 45.75 mg/g at 45 °C (Section 3.8). Whereas, the isotherm study of fresh alumina at 45 °C exhibited the Q_m of 23.42 mg/g (Fig. 16b). Hence, nitric acid treatment of alumina resulted in enhancement of Q_m from 23.42 mg/g to 45.75 mg/g. The increase in the percent fluoride removal and adsorption capacity is possibly due to the enhancement of S_{BET} of fresh alumina after nitric acid treatment which facilitates the additional active sites for fluoride ion adsorption. Hence, it can be asserted that acidification of alumina with nitric acid contributes in the enhancement of fluoride ions capture from the wastewater.

3.16. Comparative performance of nitric and hydrochloric acid treated alumina

Table 6 represents the comparative overview of nitric and hydrochloric acid treated alumina. It shows that HNO_3 acid treated alumina has better defluoridation efficiency and less equilibrium time of adsorption compared to hydrochloric acid treated alumina reported in the literature (Chen et al., 2010a). Therefore, it can be asserted that HNO_3 acid treated alumina is more advanced than HCl acid treated alumina in terms of defluoridation efficiency and treatment time.

3.17. Application of HNAA adsorbent on industrial wastewater

The characteristics of industrial wastewater utilized for defluoridation experimentation is provided in Table 7. The defluoridation performance of HNAA adsorbent on industrial wastewater is represented in Fig. 17 and Fig.S5. It demonstrates that the application of HNAA adsorbent on industrial wastewater has dropped the concentration of fluoride ions from 17.5 mg/L to 1.484 mg/L (i.e., < 1.5 mg/L, WHO permissible limit) after the contact time of 200 min (Fig. 17). The continuation of contact time up to 460 min resulted in 0.845 mg/L of fluoride ions concentration in the adsorbent treated wastewater (i.e., filtrate). It implies total 95.17% of defluoridation from the industrial wastewater (Fig.S5). The final pH of industrial wastewater after treatment with the adsorbent is found to be 6.98 ± 0.37 which comes in the range of normal usable water. The Table 7 shows the drop in the concentration of chloride, nitrate and bromide ions in the filtrate. It may be due to the adsorption on the surface of HNAA adsorbent. Besides, Table 7 also demonstrates the drop in the concentration of cations of wastewater. It is possibly due to precipitation with the freely available anions present in the wastewater. The drop in the value TOC, TDS and conductivity of the HNAA treated wastewater is also noticed after treatment with the adsorbent. It is due to the decrease of cations and anions concentration in the filtrate.

4. Conclusions

In this study, an adsorbent (HNAA) for removal of fluoride was prepared from alumina by the simple and convenient process of nitric acid activation. The SEM/EDX and BET analysis signified the successful acidic activation of alumina and adsorption of fluoride ions. The FTIR analysis revealed the role of hydroxyl and nitrate functional groups in the adsorption of fluoride ions. The point of zero charge (pH_{zpc}) of adsorbent was found to be 5.825 indicating its electropositive nature at the pH of 3.5 (i.e., optimum pH). The adsorption of fluoride ions on HNAA was better described by the Freundlich isotherm model than the Langmuir isotherm model. The isotherm study revealed that the maximum adsorption capacity of HNAA was 45.75 mg/g at 45 °C. The kinetics of fluoride adsorption was dominated by the pseudo second order kinetic model. The value of enthalpy change, Gibbs free energy change and separation factor indicated the endothermic, spontaneous and favorable adsorption, respectively. The fluoride ions adsorption on HNAA

was controlled by electrostatic attraction and ion-exchange mechanism. The carbonate and bicarbonate coexisting ions created maximum hindrance in adsorption of fluoride ions. The nitric acid activation resulted in the enhancement of defluoridation efficiency and adsorption capacity of alumina from 74.18% - 97.43% and 23.42 mg/g - 45.75 mg/g, respectively. The HNAA adsorbent also showed the potential of regeneration (> 99%) and reusability (four cycles). The application HNAA on industrial wastewater (17.5 mg/L) resulted in defluoridation less than 1.5 mg/L. Therefore, this study revealed that HNAA can be promising adsorbent for removal of fluoride ions from industrial wastewater.

Acknowledgement

The authors would like to acknowledge the Indian Institute of Technology Kharagpur for help and support during the research period.

Appendix A. Supplementary data

Supplementary material related to this article can be found, in the online version, at doi:https://doi.org/10.1016/j.jhazmat.2019.120917.

References

Fan, X., Parker, D.J., Smith, M.D., 2003. Adsorption kinetics of fluoride on low cost materials. Water Res. 37, 4929–4937.
Naim, M.M., Moneer, A.A., El-Said, G.F., 2012. Defluoridation of commercial and annular sodium fluoride solutions without using additives by batch electrocoagulation-flotation technique. Desalin. Water Treat. 44, 110–117.
Biswas, K., Gupta, K., Ghosh, U.C., 2009. Adsorption of fluoride by hydrous iron (III)-tin (IV) bimetal mixed oxide from the aqueous solution. Chem. Eng. J. 149, 196–206.
Guler, C., Thyne, G.D., 2004. Delineation of hydrochemical facies distribution in a regional groundwater system by means of fuzzy c-means clustering. Water Resour. Res. 40, W12503.
Meenakshi, Maheshwari, R.C., 2006. Fluoride in drinking water and its removal. J. Hazard. Mater. 137, 456–463.
WHO, 2006. 3rd ed. Chemical Fact Sheets: Fluoride Guidelines for Drinking Water Quality Incorporation First Addendum, vol.1. WHO, Geneva, pp. 375–377 Recommendation.
Dong, S., Wang, Y., 2016. Characterization and adsorption properties of lanthanum-loaded magnetic hydrogel composite for fluoride removal. Water Res. 88, 852–860.
Bhatnagar, A., Kumar, E., Sillanpaa, M., 2011. Fluoride removal from water by adsorbent: a review. Chem. Eng. J. 171 (3), 811–840.
Nie, Y., Hu, C., Kong, C., 2012a. Enhanced fluoride adsorption using Al(III) modified calcium hydroxyapatite. J. Hazard. Mater. 233-234, 194–199.
Asgari, G., Roshani, B., Ghanizadeh, G., 2012. The investigation of kinetics and isotherm of fluoride adsorption onto functionalize pumice stone. J. Hazard. Mater. 217-218, 123–132.
USEPA, 2003. Water treatment technology feasibility support document for chemical contamination. Support of EPA Six-year Review of National Primary Drinking Water Regulation, EPA. 815-R-03-004.
Kumar, E., Bhatnagar, A., Kumar, U., Sillanpaa, 2011. Defluoridation from aqueous solution by nano alumina: characterization and sorption studies. J. Hazard. Mater. 186, 1042–1049.
Ghorayi, S., Pant, K.K., 2004. Investigations on column of fluoride adsorption by activated alumina in fixed bed. Chem. Eng. J. 98, 165–173.
Ku, Y., Chiou, H.M., 2002. The adsorption of fluoride ion from aqueous solution by activated alumina. Water Air Soil Pollut. 133 (1-4), 349–361.
Wang, S., Zhu, Z.H., 2007. Effect of acidic treatment of activated carbons on dye adsorption. Dyes Pigm. 75, 306–314.
El-Hendawy, A.-N.A., 2003. Influence of HNO_3 oxidation on the structure and adsorptive properties of corncob-based activated carbon. Carbon 41, 713–722.
Gokce, Y., Aktas, Z., 2014. Nitric acid modification of activated carbon produced from waste tea and adsorption of methylene blue and phenol. Appl. Surf. Sci. 313, 352–359.
Dutta, M., Mishra, S., Kaushik, M., Basu, J.K., 2011. Application of various activated carbons in the adsorptive removal of methylene blue from aqueous solution. Res. J. Environ. Sci. 5 (9), 741–751.
Gong, W.X., Qua, J.H., Lia, R.P., Lan, H.C., 2012. Adsorption on different type of aluminas. Chem. Eng. J. 189-190, 126–133.
Chen, H.Wu.L., Gao, G., Zhang, Y., Wang, T., Guo, S., 2010a. Treatment effect on the adsorption capacity of alumina for removal fluoride. Nano Biomed. 2 (4), 231–235.
Kumari, U., Behera, S.K., Meikap, B.C., 2019. A novel acid modified alumina adsorbent with enhanced defluoridation property: kinetics, isotherm and applicability on industrial wastewater. J. Hazard. Mater. 365, 868–882.
Foo, K.Y., Hameed, B.H., 2012. Adsorption characteristics of industrial solid waste derived carbon prepared by microwaves heating for methylene blue. Fuel Process. Technol. 99, 103–109.
Sriprang, P., Wongnawa, S., Sirichote, O., 2014. Amorphous titanium dioxide as an adsorbent for dye pollutant water and its recyclability. J. Sol-Gel Sci. Technol. 71, 86–95.
Wang, A., Zhu, Q., Xing, Z., 2019a. Design and synthesis of a calcium modified quaternized chitosan hollow sphere for efficient adsorption of SDBS. J. Hazard. Mater. 369, 342–352.
Wang, J., Gao, M., Shen, T., Yu, M., Xiang, Y., Liu, J., 2019b. Insight into the efficient adsorption of rhodamine B on tunable organo-vermiculites. J. Hazard. Mater. 366, 501–511.
Lin, H.Y., Yuan, C.S., Chen, W.C., Hung, C.H., 2006. Determination of the adsorption isotherm of vapour phase mercury chloride on powdered activated carbon using thermogravimetric analysis. J. Air Waste Manage. Assoc. 56 (11), 1550–1557.
Siswoyo, E., Qoniah, I., Lestari, P., Fajri, J.A., Sani, R.A., Sari, D.G., Boving, T., 2019. Development of a floating adsorbent for cadmium derived from modified drinking water treatment plant sludge. Environ. Technol. Innov. 14, 100312.
Wu, T., Mao, L., Wang, H., 2017. Adsorption of fluoride from aqueous solution by using hybrid adsorbent fabricated with Mg/Fe composite oxide and alginated via a facile method. J. Fluoride Chem. 200, 8–17.
Ma, W., Chen, Y., Zhang, W., Zhao, W., 2017. Performance and mechanism of Mg-Ca-Fe hydrotalcite-like compounds for fluoride removal from aqueous solution. J. Fluorine Chem. 200, 153–161.
Adak, M.K., Sen, A., Mukherjee, A., Sen, S., Dhak, D., 2017. Removal of fluoride from drinking water using efficient nano-adsorbent, Al(III)-Fe(III)-La(III) trimetallic oxide prepared by chemical route. J. Alloys Compd. 719, 460–469.
Lu, X., Zhou, X.J., Wang, T., 2013. Mechanism of uranium (VI) uptake by *Saccharomyces cerevisiae* under environmentally relevant conditions: batch, HRTEM and FTIR studies. J. Hazard. Mater. 262, 297–303.
Hussain, Z., Daosheng, L., Xi, L., Jiangxiong, K., 2015. Defluoridation by a Mg-Al-La triple-metal hydrous oxide: synthesis, sorption, characteristics and emphasis on neutral pH of treated water. RSC Adv. 5, 43906.
Costa, T.M.H., Gallas, M.R., Benvenutti, E.V., da Jornada, J.A.H., 1999. Study of nanocrystalline Υ-Al_2O_3 produced by high pressure compaction. J. Phys. Chem. B 103, 4278–4284.
Abou, T.M.F., Mahmoud, G.A., Elsigenv, S.M., Hegazy, E.-S.A., 2008. Adsorption and desorption of phosphate and nitrate ions using quaternary (polypropylene-g-N,N-dimethylamino ethmethacrylate) graft copolymer. J. Hazard. Mater. 159, 372–379.
Layden, D.E., Collins, W.T., Surface, S., 1980. Midland Macromolecular Institute, Dow Corning Corporation. Gordon and Beacher Science Publichers, pp. 7 Chapter 1.
Wang, A., Zhou, K., Liu, X., Liu, F., Chen, Q., 2017a. Development of Mg-Al-La tri-metal mixed oxide entrapped in alginate from removal of fluoride from waste water. RSC Adv. 7, 31221–31229.
Siswoyo, E., Mihara, Y., Tanaka, S., 2014. Determination of key components and adsorption capacity of a low-cost adsorbent based on sludge of drinking water treatment plant to adsorb cadmium ions in water. Appl. Clay Sci. 97-98, 146–152.
Siswoyo, E., Tanaka, S., 2013. Development of eco-adsorbent based on solid waste of paper industry to adsorb cadmium ion in water. J. Clean Energy Technol. 1 (3), 198–201.
Clifford, D., Matson, J., Kennedy, R., 1978. Activated alumina: rediscovered adsorbent for fluoride, humic acids and silica. Ind. Water Eng. 15, 6–12.
Lima, E.C., Adebayo, M.A., Machado, F.M., 2015. Kinetics and Equilibrium Models of Adsorption, Carbon Nanomaterials As Adsorbent for Environmental and Biological Application. Springer, pp. 33–69.
Tien, C., 1994. Adsorption Calculation and Modelling. Butterworth-Heinemann, Massachusetts, USA.
Dayananda, D., Sarva, V.R., Prasad, V.S., Arunachalam, J., Ghosh, N.N., 2015. A Simple aqueous solution based chemical methodology for preparation of mesoporous alumina: efficient adsorbent for defluoridation of water. Part. Sci. Technol. 33, 8–16.
Chen, N., Zhang, Z., Feng, C., Sugiura, N., Li, M., Chen, R., 2010b. Fluoride removal from water by granular ceramic adsorption. J. Colloid Interface Sci. 348 (2), 579–584.
Pietrelli, L., 2005. Fluoride wastewater treatment by adsorption onto metallurgical grade alumina. Annal. Chim. 95 (5), 303–312.
Huang, Z., Zhou, A., Wu, J., Chen, Y., Lan, X., Bai, H., Li, L., 2016. Bottom-up preparation of ultrathin 2D aluminum oxide nanosheets by duplicating grapheme oxide. Adv. Mater. 28, 1703–1708.
Zhua, J., Lin, X., Wu, P., Zhou, Q., Luo, X., 2015. Fluoride removal from aqueous solution by Al(III)-Zr(IV) binary oxide adsorbent. Appl. Surf. Sci. 357, 91–100.
Wu, X., Zhang, Y., Dou, X., Yang, M., 2007. Fluoride removal perormace of a novel Fe-Al-Ce trimetal oxide adsorbent. Chemosphere 69, 1758–1764.
Nie, Y., Hu, C., Kong, C., 2012b. Enhanced fluoride adsorption using Al(III) modified calcium hydroxyapatite. J. Hazard. Mater. 233-234, 194–199.
Aly, Z., Graulet, A., Scales, N., Hanley, T., 2014. Removal of aluminium from aqueous solution using PAN-based adsorbents: characterisation, kinetics, equilibrium and thermodynamics studies. Environ. Sci. Pollut. Res. 21, 3972–3986.
Liu, Y., Yan, C., Zhang, Z., Wang, H., Wang, S., Zhou, S., 2016. A comparative study on fly ash, geopolymer and faujasite block for Pb removal from aqueous solution. Fuel 185, 181–189.
Fu, J., Chen, Z., Wang, M., Liu, S., Zhang, J., Han, R., Xu, Q., 2015. Adsorption of methylene blue by a high-efficiency adsorbent (polydopamine microspheres): kinetics, isotherm, thermodynamics and mechanism analysis. Chem. Eng. J. 259, 53–61.
Wang, M., Yu, X., Yang, C., Yang, X., Lin, M., Guan, L., Ge, M., 2017b. Removal of fluoride from aqueous solution by Mg-Al-Zr triple metal composite. Chem. Eng. J. 322, 246–253.
Zhou, J., Zhu, W., Yu, J., Zhang, H., Zhang, Y., Lin, X., Luo, X., 2018. Highly selective and efficient removal of fluoride from ground water by layered Al-Zr-La Tri-metal hydroxide. Appl. Surf. Sci. 435, 920–927.